Journal of
Mechanics of
Materials and Structures

WHEN BEAM THEORIES FAIL

Paul R. Heyliger

Volume 8, No. 1 January 2013

msp

JOURNAL OF MECHANICS OF MATERIALS AND STRUCTURES
Vol. 8, No. 1, 2013
dx.doi.org/10.2140/jomms.2013.8.15

WHEN BEAM THEORIES FAIL

PAUL R. HEYLIGER

The free vibration of completely unrestrained prismatic rectangular parallelepipeds and the static response of planar elastic rectangles under transverse loads are examined to determine the relative accuracy of several widely used beam theories. The Euler–Bernoulli, Rayleigh, and Timoshenko theories are applied to both isotropic and orthotropic beams and compared with elasticity-based solutions. The resulting frequencies, energies, displacements, and stresses are compared with solutions to the linear theory of elasticity for solids with the same geometries and material constitutions. Sources of the resulting differences in response are identified, and guidelines are suggested.

Introduction

The vibrating beam is one of the most studied problems in mechanics, having an extremely large number of practical applications [Timoshenko 1921; 1922; 1953; Love 1927; Anderson 1953; Traill-Nash and Collar 1953; Dolph 1954; Herrmann 1955; Huang 1961; Cooper 1966; Thomas and Abbas 1975; Abbas and Thomas 1977; Stephen 1978; 2001; Levinson 1981; King 1985; Schramm et al. 1994; Han et al. 1999; Gruttmann and Wagner 2001; Hutchinson 2001; Puchegger et al. 2003; 2005]. One of the key issues encountered when considering this problem is the loss in relative accuracy when moving from a fully three-dimensional elasticity theory to the simpler one-dimensional beam theories commonly used by most engineers. In general, the complexity of the displacement field in the beam increases as the slenderness ratio (s) of the beam decreases, where $s = L\sqrt{A/I}$, and L, A, and I represent the beam length, area of the cross-section, and second moment of the cross-sectional area, respectively. Similar behavior is found in static response for beams under a variety of loading and boundary conditions.

The most widely used beam theories in modern applications were all developed by 1921. These are the Euler–Bernoulli, Rayleigh, and Timoshenko beam theories. The excellent review of these theories (along with a rarely used shear beam model) in [Han et al. 1999] completely describes these basic theories and their behaviors under a variety of boundary conditions. There is fairly broad consensus that if the slenderness ratio is large, with the value of $s \geq 100$ used by Han and coworkers being typical, that Euler–Bernoulli theory can be used but when the slenderness ratio is "small", shear deformation models may give more accuracy.

One issue that has seen little exploration during these investigations is at what point the beam ceases to behave as such and the estimates provided by one-dimensional beam theories begin to fail. To take an extreme case, a rectangular parallelepiped with a square cross-section of sides a and length L has a slenderness ratio of $\sqrt{12}(L/a)$. For larger L/a ratios, the parallelepiped deforms according to the kinematic hypothesis consistent with Euler–Bernoulli theory, then transitions into deformation patterns

Funding from the Mountains Plains Consortium is gratefully acknowledged.
Keywords: beam, vibration, elasticity, frequency, Timoshenko, Euler–Bernoulli.

consistent with shear deformation models well represented by Timoshenko theory. But at some point, even the Timoshenko model has limitations, as L approaches and eventually takes a value less than a. What was once a beam becomes a thin square plate with thickness L and side edge lengths of a, with completely different behavior.

In this study, elasticity theory is used to determine the limits of beam-theory accuracy as the slenderness ratio decreases for both dynamic and static responses. This is accomplished first by comparing the frequency and modal displacement results from three commonly used beam theories (Euler–Bernoulli, Rayleigh, and Timoshenko) with those of approximate solutions to the equations of motion for linear elasticity for the same solid. Specific attention is paid to the simplest possible set of boundary conditions (from an elasticity perspective): the free-free beam. This translates to the problem of zero end shear and moment for the beam theories and traction-free vibration for a three-dimensional solid, and allows a direct comparison for determining, at least in part, when beam theories fail to capture the mechanics of deformation in these solids. Second, the static response of a beam under transverse sinusoidal loading is considered using beam theories and an exact linear elasticity solution. In both cases, the objective is to provide estimates of the errors induced by various beam theory approximations as the slenderness ratio decreases.

Theoretical foundation

Governing equations. For a three-dimensional solid, there are three displacement components: $u_1(x_1, x_2, x_3)$, $u_2(x_1, x_2, x_3)$, and $u_3(x_1, x_2, x_3)$. They are linked to components of infinitesimal strain via the relations

$$\epsilon_{ij} = \frac{1}{2}\left(\frac{\partial u_i}{\partial x_j} + \frac{\partial u_j}{\partial x_i}\right). \tag{1}$$

Here ϵ_{ij} are the components of the infinitesimal stain tensor and u_i represent the displacement components in indicial form. These strains are related to the components of Cauchy stress via the generalized Hooke's law, given by

$$\sigma_{ij} = C_{ijkl}\epsilon_{kl}, \tag{2}$$

where C_{ijkl} represent the components of the elastic stiffness tensor. Substituting these stresses into the equations of motion

$$\sigma_{ij,j} = \rho\frac{\partial^2 u_i}{\partial t^2} \tag{3}$$

allows for a direct representation of these equations in terms of the three displacement variables.

An alternative to a direct solution of the equations of equilibrium uses Hamilton's principle as a starting point for approximate solutions to the equations of motion. For the case of zero body force, this can be written

$$0 = -\int_0^t \int_V \{\sigma_{11}\delta\epsilon_{11} + \sigma_{22}\delta\epsilon_{22} + \sigma_{33}\delta\epsilon_{33} + 2\sigma_{23}\delta\epsilon_{23} + 2\sigma_{13}\delta\epsilon_{13} + 2\sigma_{12}\delta\epsilon_{12}\}\, dV dt + \delta\int_0^t \int_S t_i \delta u_i dS + \frac{1}{2}\delta\int_0^t \int_V \rho(\dot{u}_1^2 + \dot{u}_2^2 + \dot{u}_3^2)\, dV dt. \tag{4}$$

Here V is the volume of the solid, $\dot{u} = \partial u/\partial t$, t represents time, ρ is the density of the material, t_i are the specified surface tractions, and δ is the variational operator.

Beam theory displacement fields. The general procedure for simplifying computational models in the field of solid mechanics is to restrict the way that a general particle within the solid can deform by imposing kinematic constraints through an assumed displacement field. This can take a variety of forms, but the general intent in beam, plate, and shell theories is to reduce the dimensions of the problem and thereby simplify the subsequent analysis. In this study, each of the models used (the three beam theories and the three-dimensional elasticity solution) imposes a sequence of constraints represented in the resulting displacement fields. In the discussion that follows, the standard notations of $u_1 = u$, $u_2 = v$, and $u_3 = w$ and $x_1 = x$, $x_2 = y$, and $x_3 = z$ are both used because of clarity and common usage. The long axis of the beam is given by x and the cross-section coordinates are y in the out-of-plane direction and z in the transverse direction of the beam. Additionally, only displacement fields corresponding to bending action are considered in this study. There are of course types of beams in which the axial, torsional, and bending action are coupled [Hodges 2006; Marigo and Meunier 2006], but those cases are not considered here.

Euler–Bernoulli and Rayleigh beam theories. The Euler–Bernoulli beam is represented by a single unknown variable: the transverse displacement of the beam centroid $u_3 = w$. By further assuming that the Poisson's ratio is zero, the displacement field can be given by

$$u_1(x_1, x_2, x_3) = u(x, y, z) = -z\, dw/dx, \tag{5}$$

$$u_2(x_1, x_2, x_3) = v(x, y, z) = 0, \tag{6}$$

$$u_3(x_1, x_2, x_3) = w(x, y, z) = w(x). \tag{7}$$

The only difference between the Euler–Bernoulli and Rayleigh beam theories is that in Euler–Bernoulli theory the kinetic energy associated with the u displacement component is neglected since $\dot{u}^2$ along the axis of the beam is generally much smaller in magnitude than $\dot{w}^2$ transverse to the beam axis. The equation of motion for the Euler–Bernoulli model with density ρ, elastic modulus E, moment of inertia I, and transverse loading $q(x, t)$ can be expressed in terms of w as

$$\frac{\partial^2}{\partial x^2}\left(EI\frac{\partial^2 w}{\partial x^2}\right) + \rho\frac{\partial^2 w}{\partial t^2} = q(x, t). \tag{8}$$

Timoshenko beam theory. Timoshenko beam theory [Timoshenko 1921; 1922], also sometimes referred to as a first-order shear deformation theory because it allows for nonzero transverse shear strain, is represented by two unknown functions that represent the transverse displacement (w) and the total section rotation (Ψ) of the beam cross-section:

$$u_1(x_1, x_2, x_3) = u(x, y, z) = z\Psi(x), \tag{9}$$

$$u_2(x_1, x_2, x_3) = v(x, y, z) = 0, \tag{10}$$

$$u_3(x_1, x_2, x_3) = w(x, y, z) = w(x). \tag{11}$$

Here again the Poisson's ratio is assumed to be zero. There is a fourth beam theory, rarely used, termed

the shear theory, in which the kinetic energy associated with the displacement u is neglected. This theory is not considered in this study.

The respective displacement fields can be substituted into the strain-displacement relations and appropriate constitutive law, then the resulting displacement variables can be used in the equation(s) of motion

$$\rho A\frac{\partial^2 w}{\partial t^2} - q(x,t) = \frac{\partial}{\partial x}\Big[\kappa AG\Big(\frac{\partial w}{\partial x} - \Psi\Big)\Big], \tag{12}$$

$$\rho I\frac{\partial^2 \Psi}{\partial t^2} = \frac{\partial}{\partial x}\Big(EI\frac{\partial \Psi}{\partial x}\Big) + \kappa AG\Big(\frac{\partial w}{\partial x} - \Psi\Big), \tag{13}$$

where A is the cross-sectional area, κ is the shear correction coefficient, and G is the shear modulus. For the isotropic beam, the shear and elastic modulus are related. For the orthotropic beam, these constants are independent. In either case, these governing equations can then be solved using usual methods [Han et al. 1999].

Application and results

In this section, the displacement fields associated with beam theories and elasticity theory are applied to two fundamental problems: the free vibration of the completely unrestrained rectangular parallelepiped, and the static response of a simply supported rectangular strip under transverse load. The results obtained by various beam theories can be compared with three-dimensional elasticity theory in the first case and an exact plane elasticity solution in the second case.

Traction-free vibration of the free-free beam. Most of the analyses that use beam theory require use of dimensionless variables. For a beam of length L^*, area A^*, moment of inertia I^*, we can compute the dimensionless area $A = A^*/L^{*2}$, moment of inertia $I = I^*/L^{*4}$, density $\rho = \rho^* L^{*6}\omega_1^{*2}/(EI^*)$, and frequency $\omega_i = \omega_i^*/\omega_1^*$, where ω_i represents the i-th natural frequency of the beam in radians/second.

In terms of the three beam theories, the solution reduces to satisfaction of the equation(s) of motion along with the boundary conditions associated with zero resultant transverse shear and bending moment at the two ends. For the elasticity model, the weak form of the three equations of motion embedded within (4) must be solved for the case where the boundary conditions over the entire surface must be traction-free.

Euler–Bernoulli theory. The Euler–Bernoulli beam includes strain energy terms from axial strain and kinetic energy terms only from the transverse displacement component $w(x)$. The solution for the beam transverse displacement is given as [Han et al. 1999]

$$w(x) = C_1 \sin ax + C_2 \cos ax + C_3 \sinh ax + C_4 \cosh ax. \tag{14}$$

Here a is the dimensionless wave number that is related to the dimensionless density, area, and frequencies by

$$a^4 = \rho A\omega^2. \tag{15}$$

The end conditions consistent with the free-free beam for this theory are

$$\frac{d^3 w}{dx^3} = 0, \quad \frac{d^2 w}{dx^2} = 0. \tag{16}$$

Substitution of the displacement field into these four conditions yields the 4×4 linear system whose zero determinant provides the resulting frequencies, while the values of C_i define the mode shape of the deformed beam.

Rayleigh theory. Rayleigh theory is identical to the Euler–Bernoulli model with the exception of the addition of the kinetic energy along the beam axis. This term is often referred to as the rotary inertia, and generally results in a lowering of the frequencies compared with the Euler–Bernoulli model. The solution for the transverse displacement is now

$$w(x) = C_1 \sin a_1 x + C_2 \cos a_1 x + C_3 \sinh a_2 x + C_4 \cosh b_2 x, \tag{17}$$

where the dispersion relations identify a and b as

$$a_1 = \sqrt{\rho I \omega^2/2 + \sqrt{(\rho I \omega^2/2)^2 + \rho A \omega^2}}, \tag{18}$$

$$a_2 = \sqrt{-\rho I \omega^2/2 + \sqrt{(\rho I \omega^2/2)^2 + \rho A \omega^2}}. \tag{19}$$

The boundary conditions at each free end are given as

$$\frac{d^3 w}{dx^3} + \rho I \omega^2 \frac{dw}{dx} = 0, \quad \frac{d^2 w}{dx^2} = 0. \tag{20}$$

As before, this yields a 4×4 linear system that can be solved for the respective ω and corresponding mode shapes.

Timoshenko theory. In the Timoshenko model, the strain energy and kinetic energy consistent with the full displacement fields are considered where the spatial forms of the transverse displacement w(x) and the section rotation Ψ(x) are given as

$$\begin{Bmatrix} w(x) \\ \Psi(x) \end{Bmatrix} = \begin{Bmatrix} C_1 \\ D_1 \end{Bmatrix} \sin ax + \begin{Bmatrix} C_2 \\ D_2 \end{Bmatrix} \cos ax + \begin{Bmatrix} C_3 \\ D_3 \end{Bmatrix} \sinh ax + \begin{Bmatrix} C_4 \\ D_4 \end{Bmatrix} \cosh ax, \tag{21}$$

where the parameters a and the relations between the C_i and D_i are given in [Han et al. 1999]. The end conditions consistent with the free-free beam are

$$\frac{d^3 \Psi}{dx^3} = 0, \quad \frac{dw}{dx} - \Psi = 0. \tag{22}$$

Substitution of the displacement field into these four conditions yields the 4×4 linear system whose zero determinant provides the resulting frequencies and whose values for C_i and D_i define the mode shape of the deformed beam.

Linear elasticity theory. The problem of traction-free vibration of solids of general shape cannot usually be solved using exact methods. Instead, solutions to Hamilton's principle are sought using Ritz-based approximations for the three displacement components. The displacement fields using this form of approximation where first used in [Demarest 1971], expanded in [Ohno 1976], and refined in perhaps their most efficient form in [Visscher et al. 1991; Migliori and Sarrao 1997]. Their general form can be

expressed as

$$u_1(x_1, x_2, x_3, t) = u(x, y, z, t) = \sum_{j=1}^{n} c_j(t)\phi_j^u(x, y, z), \tag{23}$$

$$u_2(x_1, x_2, x_3, t) = v(x, y, z, t) = \sum_{j=1}^{n} d_j(t)\phi_j^v(x, y, z),$$

$$u_3(x_1, x_2, x_3, t) = w(x, y, z, t) = \sum_{j=1}^{n} e_j(t)\phi_j^w(x, y, z). \tag{24}$$

Here c, d, and e are unknown constants that depend on time, and the functions ϕ are known functions of position. This form of approximation is general, and in fact can be used for a variety of models including those functions that have only local nonzero behavior (such as finite element approximation functions) along with those that exist over the entire domain of the solid. It is the latter class that is of interest in this work. In either case, substitution of these approximations into Hamilton's principle and invocation of the assumption of harmonic motion allows the problem to be reduced into the generalized eigenvalue problem given as

$$\begin{bmatrix} K_{11} & K_{12} & K_{13} \\ K_{21} & K_{22} & K_{23} \\ K_{31} & K_{23} & K_{33} \end{bmatrix} \begin{Bmatrix} c \\ d \\ e \end{Bmatrix} = \omega^2 \begin{bmatrix} M_{11} & 0 & 0 \\ 0 & M_{22} & 0 \\ 0 & 0 & M_{33} \end{bmatrix} \begin{Bmatrix} c \\ d \\ e \end{Bmatrix}. \tag{25}$$

The elements of these matrices are given in the Appendix.

The form of the approximation functions as used in this work is taken as

$$\phi_i = x^j y^k z^l. \tag{26}$$

These functions have the appealing property of being very simple to evaluate over the domain of the parallelepiped while providing a very accurate basis to represent the various displacement components of the beam. It is also possible to use group theory to split the resulting eigenvalue problem into eight smaller problems that separate the vibrational modes according to spatial dependence of the three displacements. This topic has been extensively discussed in [Ohno 1976]. The eight groups are defined in Table 1. Similar to the displacement fields of the beam theories, this class of model confines the solution to a

Grp	Disp	x	y	z	Grp	Disp	x	y	z	Grp	Disp	x	y	z	Grp	Disp	x	y	z
	u	O	E	E		u	O	O	O		u	O	O	E		u	O	E	O
OD	v	E	O	E	OX	v	E	E	O	EY	v	E	E	E	EZ	v	E	O	O
	w	E	E	O		w	E	O	E		w	E	O	O		w	E	E	E
	u	E	E	E		u	E	O	O		u	E	E	O		u	E	O	E
EX	v	O	O	E	EV	v	O	E	O	OY	v	O	O	O	OZ	v	O	E	E
	w	O	E	O		w	O	O	E		w	O	E	E		w	O	O	O

Table 1. Groupings of approximation functions. (Grp: group; Disp: displacement.)

specific combination of polynomial forms, but in general the accuracy of this model increases rapidly as the number of terms in the series increases.

The generalized eigenvalue problem for the three-dimensional solid defined earlier gives the general form of solution for the elasticity solution of the free-free beam. Of the eight groups that represent the total beam vibration of an elastic parallelepiped with either isotropic or orthorhombic symmetry, there are four that contain what can be categorized as flexural modes, as the resulting displacement patterns reflect this class of deformation. As one of the beam dimensions grows (for example, the length in the x or axial direction, defined as L in the usual beam theories), the flexural modes become easier to excite and are among the lowest of the frequencies described by the eight symmetry groups. But in all cases used in this study, only those symmetry groupings that are associated with flexure are used to compare with the results from beam theory. Modes having to do with longitudinal shear or torsion about the beam axis, for example, are eliminated from consideration when comparing with results from one-dimensional beam theories.

As the number of terms in the series used to describe the three displacement components is increased, the accuracy in the frequencies improves. To demonstrate this behavior, we consider a beam of length 0.2 m with a square cross-section of 0.01×0.01 m. The elastic constants are taken to be those of steel, with $C_{11} = 269.231$ GPa and $C_{44} = 76.923$ GPa along with a density of $7830\,\mathrm{kg/m^3}$. In Table 2, the lowest five flexural frequencies are shown as a function of the parameter $j + k + l$, which is the summed total of all powers in (26). The results indicate an accuracy, at least for these first five modes, that is adequate to at least five figures. Similar results were found for beams with other aspect ratios.

From a full analysis of this rectangular parallelepiped, there are six zero eigenvalues corresponding to the rigid body modes of the solid, then a sequence of seven repeated frequencies that represent what are usually classified as the bending modes of the beam. The first, third, fifth, and seventh frequencies are from the groups (EY, EZ), and the second, fourth, and sixth are from the groups (OY, OZ). These frequencies are repeated since they represent bending about the y and z-axes, and are identical since the beam cross-section is square. It is not until the eighth frequency where a single mode from the group EV makes an appearance. But in general, the focus here is on the bending modes so they can be directly compared with the class of frequency derived from the beam theories.

Frequencies. The mechanics of deformation for beams changes as the slenderness ratio begins to decrease. To demonstrate the limits of beam theory, the lowest five flexural modes are computed for the three main beam theories (Euler–Bernoulli (EB), Rayleigh, and Timoshenko) and compared with the

	Sum of terms in series					
Mode	8	10	12	14	16	18
1	8088.47	8088.47	8088.47	8088.47	8088.47	8088.47
2	21949.9	21943.9	21943.8	21943.8	21943.8	21943.8
3	42147.0	42073.6	42072.7	42072.7	42072.6	42072.6
4	75581.3	68056.1	67652.5	67642.7	67642.5	67642.5
5	115478.	99316.0	97915.6	97855.6	97854.2	97854.1

Table 2. Convergence of frequencies (in radians per second) of isotropic bar with $L = 0.20$ m.

same frequencies as computed using elasticity theory for zero and nonzero Poisson's ratios. This is completed for the isotropic beam using the elastic constants of steel as listed earlier, and for the orthotropic elastic constants of graphite-magnesium given as $C_{11} = C_{22} = 28.18$ (all in GPa), $C_{33} = 174.3$, $C_{12} = 10.67$, $C_{13} = C_{23} = 12.20$, and $C_{66} = 8.76$, with a density of $1738\,\mathrm{kg/m^3}$ [Ledbetter et al. 1989]. The results are given in radians/second and are all computed using a fixed cross-sectional dimension (0.01×0.01) with the length varying to give the specified slenderness ratio. The results are shown in Table 3 for the isotropic beam and Table 4 for the orthotropic beam.

	EB	Rayleigh	Timoshenko	$\nu = 0$	Full
	816033.	570862.	515972.	514674.	516233.
	2249460.	1243978.	865076.	858577.	862774.
$L = 0.02\,\mathrm{m}$	4409820.	2024066.	1220600.	1245000.	1227690.
$(s = 6.928)$	7289660.	2839420.	1226500.	1266740.	1238280.
	10889500.	3666503.	1623750.	1297740.	1383700.
	130565.	120943.	115643.	115547.	115773.
	359914.	308040.	270703.	270111.	271519.
$L = 0.05\,\mathrm{m}$	705571.	553822.	450802.	449397.	452726.
$(s = 17.32)$	1166350.	836851.	635424.	633014.	638419.
	1742330.	1143697.	816534.	813070.	819523.
	32641.3	31988.3	31534.8	31526.1	31546.3
	89978.5	86145.8	82081.1	82008.3	82180.9
$L = 0.10\,\mathrm{m}$	176393.	164062.	149833.	149599.	150167.
$(s = 34.64)$	291586.	262124.	228803.	228303.	229548.
	435581.	376983.	314906.	314056.	316225.
	8160.33	8188.69	8087.68	8087.07	8088.47
	22494.6	22243.4	21396.1	21930.1	21943.8
$L = 0.20\,\mathrm{m}$	44098.2	43263.8	42042.2	42019.3	42072.6
$(s = 69.28)$	72896.6	70825.6	67562.6	67504.0	67642.5
	108895.	104599.	97688.3	97569.4	97854.1
	2040.08	2037.48	2035.50	2035.46	2035.55
	5623.65	5607.75	5587.49	5587.09	5588.01
$L = 0.40\,\mathrm{m}$	11024.5	10971.3	10887.3	10885.7	10889.5
$(s = 138.56)$	18224.1	18090.5	17854.5	17849.9	17860.4
	27223.8	26943.0	26413.3	26403.2	26426.6
	326.413	326.350	326.299	326.298	326.300
	899.785	899.373	898.847	898.837	898.861
$L = 1.0\,\mathrm{m}$	1763.93	1762.56	1760.35	1760.31	1760.41
$(s = 346.4)$	2915.86	2912.42	2906.10	2905.97	2906.26
	4355.81	4348.52	4334.06	4333.77	4334.42

Table 3. Frequencies for isotropic bar with rectangular cross-section.

Several broad observations can be made. The widely used assumption of zero Poisson's ratio as used within an isotropic elasticity model results in frequencies that are nearly always below the exact values with the full elastic constants. This difference is less than one percent for the lowest five modes for slenderness ratios at or above 17 for both the isotropic and orthotropic beams. For slenderness ratios less than about 10, this behavior transitions to less consistent behavior with the differences in frequency rapidly increasing to over 10 percent for some values. However, for most cases, the assumption of no Poisson's effect has a very small influence on the resulting frequency spectra.

	EB	Rayleigh	Timoshenko	$\nu = 0$	Full
	1581020.	1106017.	674806.	769102.	769967.
	4358220.	2410141.	801592.	944903.	957027.
$L = 0.02\,\mathrm{m}$	8543800.	3921528.	1155010.	961637.	959906.
$(s = 6.928)$	14123400.	5501235.	1416310.	1039640.	1051190.
	21097900.	7103668.	1750170.	1283550.	1281090.
	252964.	234321.	189850.	201500.	201793.
	697315.	596813.	359106.	405631.	406741.
$L = 0.05\,\mathrm{m}$	1367010.	1073002.	532576.	617063.	618665.
$(s = 17.32)$	2259740.	1621357.	677543.	804311.	805812.
	3375670.	2215856.	857382.	944903.	953822.
	63240.9	61975.8	57667.4	58930.7	58963.2
	174329.	166903.	133924.	142312.	142532.
$L = 0.1\,\mathrm{m}$	341752.	317862.	219221.	240694.	241250.
$(s = 34.64)$	564934.	507852.	304759.	343250.	344205.
	843917.	730385.	389128.	446464.	447792.
	15810.2	15729.6	15417.8	15513.5	15516.0
	43582.2	43095.6	40177.8	41031.6	41053.8
$L = 0.2\,\mathrm{m}$	85438.0	83821.4	73087.0	76023.5	76100.9
$(s = 69.28)$	141234.	137221.	110850.	117535.	117713.
	210979.	202655.	151253.	163291.	163610.
	3952.56	3947.52	3927.23	3933.52	3933.71
	10895.6	10864.7	10660.9	10723.5	10725.1
$L = 0.4\,\mathrm{m}$	21359.5	21256.4	20431.9	20680.0	20686.4
$(s = 138.56)$	35308.4	35049.5	32803.4	33461.6	33478.8
	52744.8	52200.7	47342.1	48721.7	48758.0
	632.409	632.287	631.761	631.926	631.930
	1743.29	1742.49	1737.09	1738.78	1738.82
$L = 1.0\,\mathrm{m}$	3417.52	3414.87	3392.30	3399.31	3399.45
$(s = 346.4)$	5649.34	5642.66	5578.50	5598.35	5598.86
	8439.17	8425.05	8279.24	8324.08	8325.23

Table 4. Frequencies for anisotropic bar with rectangular cross-section.

The decision to use an Euler–Bernoulli beam theory versus Rayleigh theory is, at least for modern practical applications, rarely an issue. Most analysts will use finite element models in which the rotary inertia is incorporated into the mass matrix of the finite element equations. In general the Rayleigh results are lower than those of Euler–Bernoulli theory since the additional kinetic energy terms from the rotary inertia effectively appear on the same side as the frequency in the eigenvalue equation. For the beams considered in this study, the differences in frequency obtained from these two theories is quite small when the beam is very slender (s over 100), with changes that increase with mode number that also dramatically differ when the beam becomes thick (with s under 50). There is not a significant difference between the isotropic and anisotropic beam behavior in this regard. However, the higher-mode Rayleigh frequencies are larger than the elasticity values by up to several percent even when the beam is very slender (s over 100). For a beam of dimensions $1 \times 1 \times 20$ ($s = 69.28$), the errors in the lowest five frequencies range from 0.7 to 8 percent for the isotropic beam and 1.6 to 25 percent for the orthotropic beam, with the higher modes having the larger errors. When the beam is $1 \times 1 \times 10$ ($s = 34.64$), the errors range from 2.55 to 23 percent for the isotropic case and 6.3 to 69 percent for the orthotropic beam. Hence although the fundamental frequency of the Rayleigh beam yields good agreement with elasticity results, the decision to use either of these two theories to predict higher modes is of questionable merit. This would of course be even more true if these elements are used to consider assemblies of beams into a planar or spatial frame.

The Timoshenko beam model provides excellent agreement with elasticity results for the case of the isotropic beam. For this study, the shear correction coefficient was taken to be 0.85 [Han et al. 1999], which is a well-established value for isotropic and rectangular cross-sections. The fundamental bending mode is well within a single percent of the full elasticity results for virtually all cases, even when the beam becomes very thick. For more realistic slenderness ratios, the first five modes match very well even for relatively stocky beams. For larger slenderness ratios, the frequencies provided by the Timoshenko model are in between the elasticity solutions for zero and nonzero Poisson's ratio results, and this appears to hold for all of the five lowest bending frequencies. It is only when the slenderness ratio is less than about 10 that the higher modes become less accurate.

For the orthotropic beam, the Timoshenko model appears to be significantly less robust. The shear correction coefficient value was taken to be 0.8406 in the case of these material properties, and was computed according to the method of [Puchegger et al. 2003; 2005]. There have been far fewer studies of shear correction coefficients for orthotropic beams than for the isotropic case, in part because of the wide variability that can exist between the longitudinal and shear moduli for some materials. Once again, the assumption of zero Poisson's ratio has negligible influence on the results. Most of the frequencies computed using the full stiffness tensor are only slightly (far less than one percent) higher than the frequencies computed using the assumption of zero Poisson's ratio. The anisotropic Timoshenko theory also does a reasonable job predicting the fundamental bending frequency for moderately stocky beams. However, unlike the isotropic theory, the errors become significant when the slenderness ratio reaches lower double digits (roughly $s = 20$). Additionally, Timoshenko theory does not do as well with higher modes even when the beam is quite thin. Errors between the elasticity and Timoshenko theory for the first five modes are 0.17, 0.60, 1.2, 2.1, and 3.0 percent when the beam dimensions are $1 \times 1 \times 40$, with the Timoshenko model underpredicting the frequencies. When the beam is $1 \times 1 \times 20$, these errors jump to 0.64, 2.2, 4.1, 6.2, and 8.2 percent. For a $1 \times 1 \times 10$ beam, they are 2.2, 6.4, 10.0, 12.9, and

15.1 percent. These differences are far more significant than for the isotropic case, suggesting that a single shear coefficient has difficulty capturing the total energy contribution from higher modes when the material is anisotropic.

Mode shapes. The mode shapes for the beam theories and the elasticity theory are easily computed using the solution of the respective eigenvalue problems. The distorted shapes of the lowest five modes are shown in Figure 1 for slenderness ratios of 69.28 (a $1 \times 1 \times 20$ beam) and 6.928 (a $1 \times 1 \times 2$ beam) for

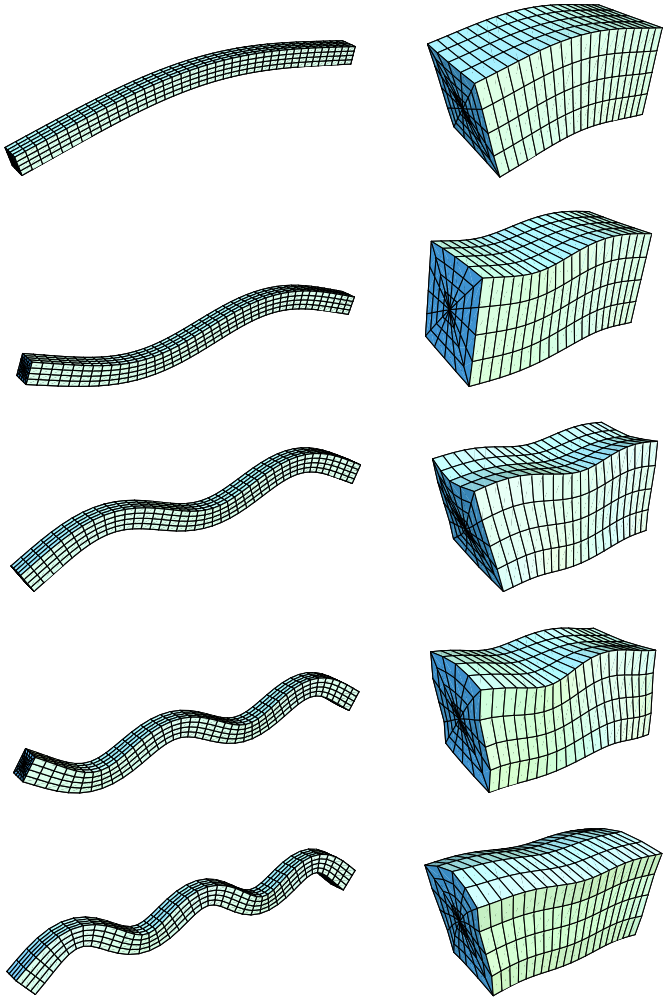

Figure 1. The first five mode shapes for the isotropic beam change in character as the slenderness ratio decreases, shown here as computed by elasticity theory. On the left, the modes for relative dimensions of $1 \times 1 \times 20$ ($s = 69.28$) are well represented by the beam theories, and plots of the transverse displacement are virtually identical to those for all three beam theories and elasticity theory. On the right, with a geometry of $1 \times 1 \times 2$ ($s = 6.928$), significant changes are apparent, with curved lines through the thickness and surfaces that possess significant warping.

isotropic material properties. Usually these modes are plotted using only the transverse displacement w for the beam theories (along with the section rotation for Timoshenko theory) but in this case we have plotted the entire solid. For the slender beam, there is no visible difference between the transverse displacement pattern between the elasticity and beam theory results, and the deformation field is significant in that the entire surfaces of the beam remain relatively smooth. In fact, one can see that the plane sections of the beam are remaining flat and are deforming very close to the assumptions of the Euler–Bernoulli and Rayleigh theories.

For the thicker beam, there are significant changes in behavior for these modes. The lowest mode shape is very similar to that of the thin beam, but as the modes progress in order there is an increasingly large deviation from the smooth-faced behavior of the slender beam. There is not only distortion of the vertical lines representing the plane deformation, but there are indications of warping across the top surfaces along with a total deformation field that is difficult to capture using only one or two variables. The case of $s = 6.928$ is somewhat extreme, but the transition from slender beam behavior to vibrating solid behavior is the crucial aspect of this work.

These plots give an indication of the visual difference between behaviors, but other metrics can be used to reinforce the sources of the changes in frequency. Because so much of the deformation is comprised of the axial stretch along the length of the beam, it is useful to consider the changes in the deformation pattern as the modes increase and the slenderness ratio decreases. Figure 2 shows the contours of the axial displacement for the upper right quadrant of the beam for the lowest five modes of the isotropic beam with stocky geometry ($1 \times 1 \times 5$ and $1 \times 1 \times 2$). The contours associated with all three beam theories are not shown but they are easy to visualize: they would be perfectly straight horizontal lines spaced an equal distance in the vertical direction (see the form of the axial displacement component u for the beam theories, which all linearly depend on z but have no spatial dependence on the other cross-sectional component).

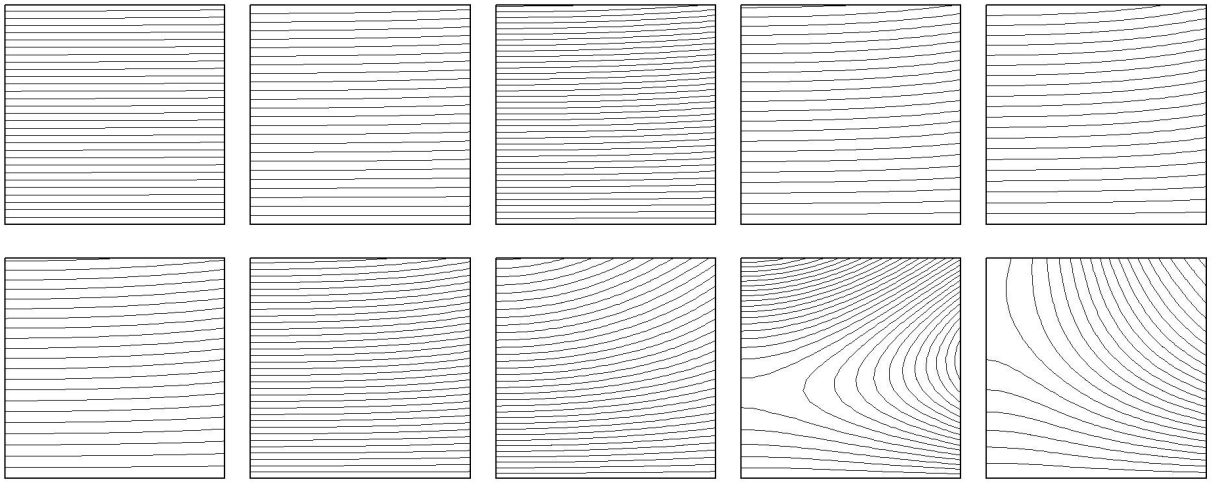

Figure 2. These contour plots show the upper right quadrant of the axial displacement for the isotropic beam computed using elasticity theory for lengths of 0.05 (top) and 0.02 (bottom). The lowest modes are on the left. They demonstrate the breakdown of beam theory approximations which assume that these components are linear in z.

These figures clearly show how the assumption of single-power displacement fields can be adequate for low-mode, high-s vibrations. In fact, even the fundamental mode for $s = 17.32$ is well captured by such an assumption. But as the mode number increases, the displacement field becomes nonlinear in the horizontal coordinate direction of the beam cross-section, and the displacement fields for the low-s beams diverge even more strongly. They indicate that a slightly more inclusive displacement field, perhaps with a small number of additional terms dependent on the $x_2 = y$ coordinate, could better capture this basic behavior.

Kinetic and strain energy. The goal of most beam theories is to be able to mimic the actual behavior of a solid using as few variables as possible. Since the natural frequencies of a vibrating solid are dependent on the ability of these theories to capture both the kinetic and strain energies corresponding to each mode shape, the sources of error when compared with elasticity solutions can be determined and potentially eliminated using more sophisticated kinematic assumptions.

The strain energy density U_o at any point in the solid can be expressed as

$$U_o = U_o^{11} + U_o^{22} + U_o^{33} + U_o^{23} + U_o^{13} + U_o^{12} = \tfrac{1}{2}\sigma_{11}\epsilon_{11} + \tfrac{1}{2}\sigma_{22}\epsilon_{22} + \tfrac{1}{2}\sigma_{33}\epsilon_{33} + \sigma_{23}\epsilon_{23} + \sigma_{13}\epsilon_{13} + \sigma_{12}\epsilon_{12}, \quad (27)$$

and the kinetic energy density can be expressed as

$$K = K_o^{11} + K_o^{22} + K_o^{33} = \tfrac{1}{2}\rho\dot{u}_1^2 + \tfrac{1}{2}\rho\dot{u}_2^2 + \tfrac{1}{2}\rho\dot{u}_3^2. \quad (28)$$

These scalar functions of position can be integrated over the domain of the beam to give the strain energy and kinetic energy associated with any displaced shape of the beam. For example, we can define

$$K^{11} = \int_V K_o^{11}\, dV. \quad (29)$$

Hence K^{11} is simply the size of the kinetic energy term along the axis of the beam for a specific modal deformation pattern. Using this separation and the modal displacement patterns that result from the solution of the eigenvalue problem, it is a simple matter to separate the relative contribution of each displacement component and stress-strain contribution to the total kinetic and strain energies for each mode. This allows an assessment of the sources of error between elasticity theory and the beam theories.

The influence of each term is shown by computing the relative size of the contribution of each of the terms from the kinetic and strain energy terms for the first five modes considered in the earlier examples. Since the amplitude of each mode is arbitrary, the values are normalized with respect to the dominant terms in the kinetic (K^{33}) and strain (U_{11}) energies. These terms are selected as the reference values since for flexural modes most of the energy associated with the motion is transverse for the kinetic term and axial for the strain term. Hence for each mode the amplitudes of motion are scaled so that the other terms are relative to the dominant values.

Results are shown in Figure 3 for the case of strain energy and Figure 4 for the case of kinetic energy. In Figure 3, the results are given in terms of the transverse shear strain energy scaled by the axial strain energy as a function of beam length for the isotropic and orthotropic cases. In Figure 4, the results are given in terms of the axial kinetic energy scaled by the transverse kinetic energy as a function of beam length. The contributions of all other terms are consistently several orders of magnitude lower than those of these two dominant terms and it would make little sense to modify existing beam theories to better capture these terms. They were not plotted here. The transverse kinetic energy (K^{33}) and axial strain

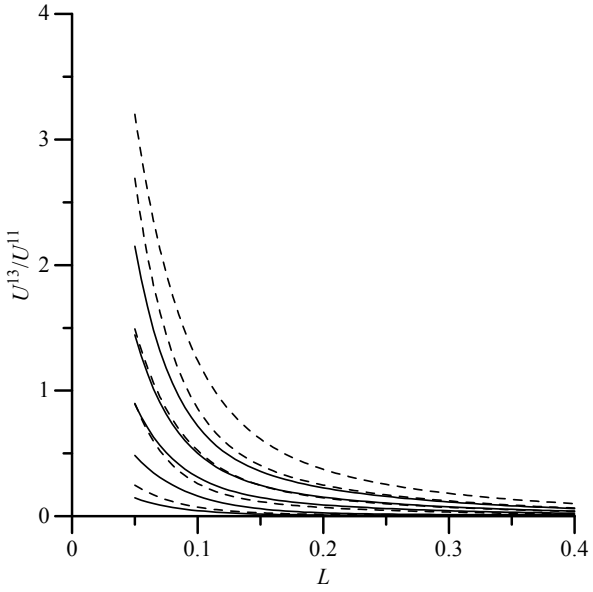

Figure 3. The ratio of the transverse shear energy to the axial energy is shown for the 0.01×0.01 beam as a function of beam length for the first five modes of the isotropic (solid lines) and orthotropic (dashed) beams. This ratio increases with mode number and is significantly more pronounced for the orthotropic beam.

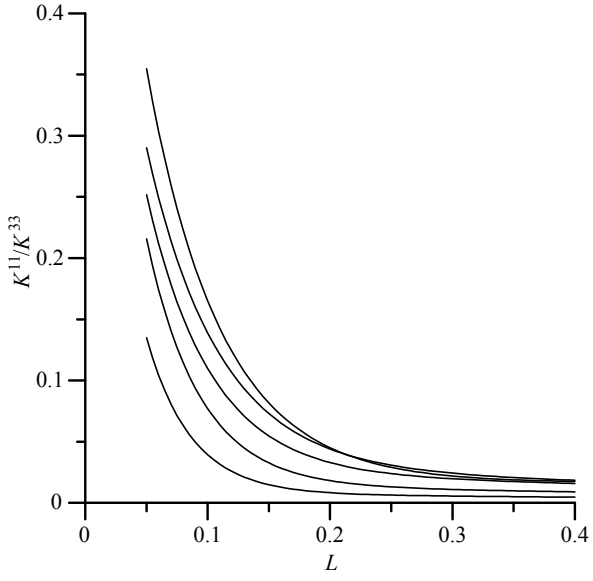

Figure 4. The ratio of the axial kinetic energy to the transverse kinetic energy is shown for the 0.01×0.01 beam as a function of beam length for the first five modes of the isotropic beam. This ratio generally increases with mode number but for most reasonably sized beams is less than five percent of the total contribution.

energy (U^{11}) dominate the total kinetic and strain energies for all thin beams. The shear strain energy contribution is larger than the rotary kinetic contribution by a factor of roughly 2–5 for the isotropic case and roughly 5–10 times higher for the orthotropic beam.

In addition to the tabulated results, the ratios of the energies as computed using elasticity theories to those of Timoshenko theory were also computed. The ratios of the transverse kinetic energy of the isotropic beam computed by elasticity theory to that of Timoshenko theory when the maximum displacements are the same are given by 0.9996, 0.9996, 0.9997, 1.00001, and 1.0013 for beams of length 1, 0.4, 0.2, 0.1, and 0.05, respectively. For the orthotropic beam, these ratios are 0.99914, 1.0013, 1.0061, 1.0234, and 1.079. The ratios of the axial strain energies for the lowest modes of the isotropic beam (again with $L = 1.0, 0.4, 0.2, 0.1$, and 0.05) are 1.000004, 1.000024, 1.000099, 1.0004, and 1.0018, respectively. The axial kinetic energy ratios (elasticity over Timoshenko) are 0.99983, 0.99986, 0.999993, 1.0005, and 1.0025. However, for the orthotropic beam the axial strain energy ratios are 1.00079, 1.0049, 1.0194, 1.0737, and 1.256. For the axial kinetic energy, the ratios are 1.00115, 1.0081, 1.0322, 1.122, and 1.417.

Static response. The static response of a simply supported beam of length L under sinusoidal transverse loading $q(x) = q_o \sin(\pi x/L)$ is an extremely well-known problem that can also be used to compare beam theories with elasticity solutions. A beam under plane stress has the elastic constants E_1, E_3, G_{13}, and ν_{13} and has a base width of b and a height of h, with the area and second moment of area being given by $A = bh$ and $I = bh^3/12$.

Euler–Bernoulli theory. The governing equation (8) can be readily solved under the boundary conditions of $w = 0$ and $d^2w/dx^2 = 0$ at $x = 0$ and $x = L$ to give

$$w(x) = \frac{q_o L^4}{\pi^4 EI} \sin \frac{\pi x}{L}. \tag{30}$$

Here $E = E_1$, which is simply the elastic modulus along the beam axis. The other elastic constants play no role in the one-dimensional response for this theory.

Timoshenko theory. An exact Timoshenko solution can be obtained by substituting the assumed solution

$$w(x) = C_1 \sin \frac{\pi x}{L}, \quad \Psi(x) = C_2 \cos \frac{\pi x}{L}, \tag{31}$$

into the governing equations (12) and (13). This results in the solution of the linear system

$$\begin{bmatrix} kGA\dfrac{\pi^2}{L^2} & kGA\dfrac{\pi}{L} \\ kGA\dfrac{\pi}{L} & kGA + EI\dfrac{\pi^2}{L^2} \end{bmatrix} \begin{Bmatrix} C_1 \\ C_2 \end{Bmatrix} = \begin{Bmatrix} q_o \\ 0 \end{Bmatrix}. \tag{32}$$

Here $G = G_{13}$, where now the beam response is a function of the two elastic constants E and G. This is true for both the isotropic and anisotropic cases.

Plane elasticity solution. A solution that is exact within the constraints of plane stress can also be obtained for this problem. This is in fact a special case of the exact solution obtained in [Pagano 1969]. The equilibrium equations in the x and z directions for a beam/strip along the x-axis of length L and

height in z of h can be expressed as

$$C_{11}\frac{\partial^2 u}{\partial x^2}+C_{13}\frac{\partial^2 w}{\partial x\partial z}+C_{55}\frac{\partial^2 u}{\partial z^2}+C_{55}\frac{\partial^2 w}{\partial x\partial z}=0, \tag{33}$$

$$C_{55}\frac{\partial^2 w}{\partial x^2}+C_{55}\frac{\partial^2 w}{\partial x\partial z}+C_{33}\frac{\partial^2 u}{\partial z^2}+C_{13}\frac{\partial^2 w}{\partial x\partial z}=0. \tag{34}$$

Here the elastic constants are obtained by inverting the compliance matrix under plane stress conditions (which contains E_1, E_3, G_{13}, and ν_{13}) to obtain the reduced stiffnesses C_{11}, C_{33}, C_{13}, and C_{55}.

The displacement field can be assumed as

$$u(x,z)=A\cos\frac{\pi x}{L}\exp\lambda z,\quad w(x,z)=B\sin\frac{\pi x}{L}\exp\lambda z. \tag{35}$$

Substituting these into equilibrium yields the matrix expression

$$\begin{bmatrix} C_{55}\lambda^2-C_{11}\left(\frac{\pi}{L}\right)^2 & \lambda\frac{\pi}{L}(C_{13}+C_{55}) \\ -\lambda\frac{\pi}{L}(C_{13}+C_{55}) & C_{33}\lambda^2-C_{55}\left(\frac{\pi}{L}\right)^2 \end{bmatrix}\begin{Bmatrix} A \\ B \end{Bmatrix}=\begin{Bmatrix} 0 \\ 0 \end{Bmatrix}. \tag{36}$$

The values for λ can be obtained by taking the determinant of the 2×2 matrix for given elastic constants and beam length and setting the result to zero.

For isotropic beams, the four C_{ij} are reduced to two independent constants, and there are two repeated roots for λ. The solutions are given by

$$u(x,z)=\cos\frac{\pi x}{L}[(A_1+A_2z)\exp\pi z/L+(A_3+A_4z)\exp-\pi z/L], \tag{37}$$

$$w(x,z)=\sin\frac{\pi x}{L}[(B_1+B_2z)\exp\pi z/L+(B_3+B_4z)\exp-\pi z/L]. \tag{38}$$

Here the constants B_i are related to the constants A_i via

$$B_1=A_1-\frac{3C_{11}-C_{13}}{C_{11}+C_{13}}\frac{L}{\pi}A_2,\qquad B_2=A_2, \tag{39}$$

$$B_3=-A_3-\frac{3C_{11}-C_{13}}{C_{11}+C_{13}}\frac{L}{\pi}A_4,\qquad B_4=-A_4. \tag{40}$$

For the orthotropic beam, the four roots for λ_i are generally distinct and depend on the specific set of elastic constants. The displacements can be expressed as

$$u(x,z)=\cos\frac{\pi x}{L}[A_1\exp\lambda_1 z+A_2\exp\lambda_2 z+A_3\exp\lambda_3 z+A_4\exp\lambda_4 z], \tag{41}$$

$$w(x,z)=\sin\frac{\pi x}{L}[B_1\exp\lambda_1 z+B_2\exp\lambda_2 z+B_3\exp\lambda_3 z+B_4\exp\lambda_4 z], \tag{42}$$

where now the constants are related via

$$B_i=\frac{C_{11}(\pi/L)^2-C_{55}\lambda^2}{\lambda(\pi/L)(C_{13}+C_{55})}A_i. \tag{43}$$

In either case, the four constants are evaluated using the four boundary conditions on the tractions at the lower and upper surfaces of the beam. The bottom surface is traction free, and the condition at the upper surface is $\sigma_{zz}=q(x)$. The stresses can be readily computed using the appropriate constitutive law.

Displacements. In the discussion that follows, both isotropic and orthotropic constitutive laws are used. In the case of isotropic beams, the Poisson's ratio is assumed to be equal to 0.3 and the resulting displacements and stresses are compared relative to the results determined by Euler–Bernoulli theory that depend only on the elastic modulus. For the orthotropic case, the material properties used are taken as $E_1 = 155$, $E_3 = 12.1$, $G_{13} = 4.40$ (all in GPa), and $\nu_{13} = 0.248$. These values are typical of a graphite-polymer composite [Hyer 1998].

The maximum displacement at the center of the beam can be used as a single point of comparison to determine relative levels of error in beam theory assumptions. This is shown in Figure 5 for the isotropic and orthotropic beams. Only the Timoshenko and elasticity solutions are plotted since the dimensionless displacement from the Euler–Bernoulli model does not depend on length. The results are shown over the key region from $L/h = 4$ to $L/h = 12$, which corresponds to a range of slenderness ratio of roughly 14–40.

As was the case for free vibration, there is again excellent agreement between the elasticity and Timoshenko models for this fundamental behavior. The isotropic Timoshenko beam has displacements that are slightly above those of the elasticity results, while the orthotropic Timoshenko beam varies from being slightly below elasticity for larger lengths to slightly above for shorter beams. The more dramatic leap is the distinction between Euler–Bernoulli theory for isotropic versus orthotropic beams. For slenderness ratios in the low double-digits, Euler–Bernoulli theory underpredicts the displacement by a factor of between 1.5 and 3. For the isotropic beam, there is not nearly this level of discrepancy, with a maximum difference of less than 20 percent.

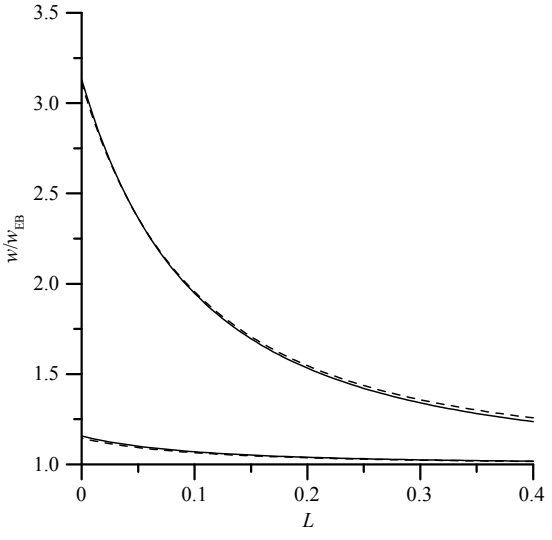

Figure 5. The ratio of the maximum transverse displacement at the beam center as computed by Timoshenko (solid) and elasticity (dashed) theories over the Euler–Bernoulli prediction is shown for the isotropic (lower curves) and orthotropic (upper curves) beams under static loading for a 1×1 beam as a function of beam length.

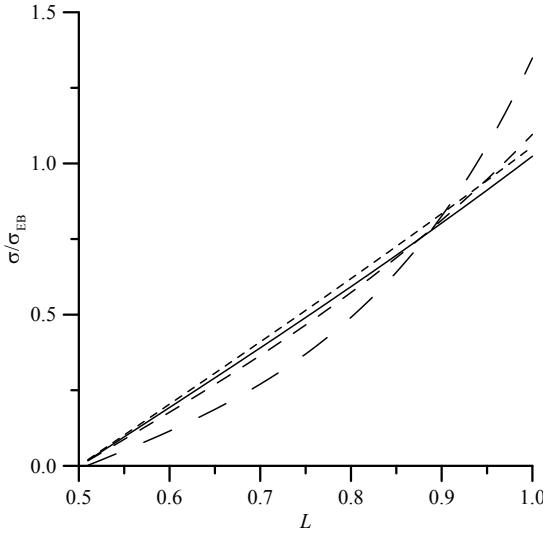

Figure 6. The ratio of the through-thickness distribution of axial stress σ_{xx} is shown over the upper half of the isotropic beam using the elasticity solution for $L = 4$ (solid) and the orthotropic beam for $L = 4$ (long dash), $L = 8$ (medium dash), and $L = 20$ (long dash). The response of the Timoshenko beam is essentially identical to the isotropic case even when the beam is short.

The longitudinal modulus is larger than the shear modulus by a factor of 2.6 for the isotropic beam but by a factor of over 35 for the orthotropic beam. As the beam becomes shorter and shear deformations accumulate, a softer shear modulus will yield much larger levels of shear deformation that cannot be captured by purely axial stiffness.

Stress. The distribution of the bending stress σ_{xx} for several cases is shown in Figure 6 for the upper half of the beam (here a beam of unit depth $h = 1$ was used). Both Euler–Bernoulli and Timoshenko theories give a distribution that is linear in z, and the question becomes how much the exact elasticity solution varies from this behavior. This figure shows that the assumption of linear variation is quite sound except for in the case of thick beams (s less than about 30), where the distribution begins to go nonlinear. For lengths of 20, 8, and 4 the elementary theory underpredicts this stress by 6, 10, and 35 percent in the orthotropic case. The isotropic beam has much smaller error, with a length of 4 giving only 2 percent error at the extreme locations of the beam cross-section. The Timoshenko beam does a very good job of capturing the maximum values of transverse shear stress regardless of aspect ratio or material constitution.

Conclusions

For the small number of cases considered here, we conclude the following:

(1) For both the isotropic and orthotropic beams, the assumption of zero Poisson's ratio has an extremely small influence. This is true for all modes and nearly all slenderness ratios explored using elasticity theory.

(2) When s is less than 100, Euler–Bernoulli theory is not competitive. For orthotropic beams, significant errors (over a single percent) appear, especially for higher modes, even when this ratio is over 100.

(3) The inclusion of the rotary inertia terms in the kinetic energy within Rayleigh theory offers only marginal improvement over the Euler–Bernoulli model. These differences are consistent with errors that are small (several percent at $s = 100$ for the isotropic case) but rapidly increase to over ten percent when s drops to low double digits and the mode number increases. For the orthotropic case, the errors are significant even at $s = 50$.

(4) For an isotropic beam with a relatively small ratio (under 3 in this case) between the axial modulus and the shear modulus, Timoshenko theory is extremely robust even as the slenderness ratio approaches single digits. For $s = 7$ (which represents a beam that is $1 \times 1 \times 2$), the lowest four frequencies are within a single percent error.

(5) For the orthotropic beam with a relatively large ratio (approximately 13 in this case) between the axial modulus and the shear modulus, Timoshenko theory generates significant errors even for beams that are relatively slender ($s = 50$), with even the fundamental frequency having an error well over a percent and even larger errors (up to 8 percent) for the higher modes. For stocky beams ($s = 10$ or so), errors are well into double digits for most of the frequencies.

(6) Rayleigh theory overpredicts the contribution of axial kinetic energy, but the lack of shear deformation restricts the relative motion and the resulting frequencies are above those of elasticity theory even for relatively high values (mid double-digit) of s.

(7) The isotropic Timoshenko beam is extremely accurate in capturing the relative axial kinetic energy contribution but underpredicts the contribution to transverse shear strain energy, leading to frequencies that are slightly below those of elasticity theory. For orthotropic Timoshenko beams, the axial kinetic energy is underpredicted and the strain energy contributions are overpredicted, with frequencies below those of elasticity theory.

(8) Under static response, isotropic beams modeled using Euler–Bernoulli theory underpredict maximum displacements by up to 20 percent for relatively thick beams but by a factor of about 3 for the orthotropic case.

(9) Static axial stress fields for isotropic beams are captured well by both Euler–Bernoulli and Timoshenko theories, even when the beam is relatively thick. Orthotropic beams generate an axial stress that goes nonlinear over the cross-section at a much higher aspect ratio, with errors of over 25 percent for $L/h = 4$.

Returning to the title, when, in fact, do beam theories fail? For isotropic materials, one potential answer is this: earlier (that is, at larger values of s) than one might expect for Euler–Bernoulli and Raleigh theories, and later (that is, at smaller values of s) than one might expect for Timoshenko theory. Given that many studies use these beam theories to predict the resonant modes for assemblies of beam/frame elements for beam geometries that possess moderately low values of s, these errors could accumulate to cast doubt on the overall accuracy of such approaches.

For orthotropic beams with high ratios of elastic to shear moduli, the answer is even more dire: one-dimensional theories generate significant errors in vibrational response even at high values (over 100)

of s. This is true even to the point that there appears to be room for adjustments or wholesale revisions of these basic theories when the material is anisotropic. Given the discrepancy between the axial kinetic and strain energy values between elasticity and Timoshenko theories, it would not be unreasonable to modify the axial displacement component as a next step in applying beam theory to the class of orthotropic beams. But one result is clear: caution should be applied in interpreting results obtained by applying beam theories to problems where higher modes, energy, or stresses are of significant interest.

Appendix

Elasticity theory. The elements of the coefficient matrices are a function of the elastic constants C_{ij} and the Ritz approximation functions ϕ, for which the superscripts indicate the variable to which that function is linked. These entries are given as

$$K_{ij}^{11} = \int_V \left(C_{11} \frac{\partial \phi_i^u}{\partial x} \frac{\partial \phi_j^u}{\partial x} + C_{55} \frac{\partial \phi_i^u}{\partial z} \frac{\partial \phi_j^u}{\partial z} + C_{66} \frac{\partial \phi_i^u}{\partial y} \frac{\partial \phi_j^u}{\partial y} \right) dV,$$

$$K_{ij}^{12} = \int_V \left(C_{12} \frac{\partial \phi_i^u}{\partial x} \frac{\partial \phi_j^v}{\partial y} + C_{66} \frac{\partial \phi_i^u}{\partial y} \frac{\partial \phi_j^v}{\partial x} \right) dV = K_{ji}^{21},$$

$$K_{ij}^{13} = \int_V \left(C_{13} \frac{\partial \phi_i^u}{\partial x} \frac{\partial \phi_j^w}{\partial z} + C_{55} \frac{\partial \phi_i^u}{\partial z} \frac{\partial \phi_j^w}{\partial x} \right) dV = K_{ji}^{31},$$

$$K_{ij}^{22} = \int_V \left(C_{22} \frac{\partial \phi_i^v}{\partial y} \frac{\partial \phi_j^v}{\partial y} + C_{44} \frac{\partial \phi_i^v}{\partial z} \frac{\partial \phi_j^v}{\partial z} + C_{66} \frac{\partial \phi_i^v}{\partial x} \frac{\partial \phi_j^v}{\partial x} \right) dV,$$

$$K_{ij}^{23} = \int_V \left(C_{23} \frac{\partial \phi_i^v}{\partial y} \frac{\partial \phi_j^w}{\partial z} + C_{44} \frac{\partial \phi_i^v}{\partial z} \frac{\partial \phi_j^w}{\partial y} \right) dV = K_{ji}^{32},$$

$$K_{ij}^{33} = \int_V \left(C_{33} \frac{\partial \phi_i^w}{\partial z} \frac{\partial \phi_j^w}{\partial z} + C_{44} \frac{\partial \phi_i^w}{\partial y} \frac{\partial \phi_j^w}{\partial y} + C_{55} \frac{\partial \phi_i^w}{\partial x} \frac{\partial \phi_j^w}{\partial x} \right) dV,$$

$$M_{ij}^{11} = M_{ij}^{22} = M_{ij}^{33} = \int_V \psi_i \psi_j \, dV.$$

References

[Abbas and Thomas 1977] B. A. H. Abbas and J. Thomas, "The second frequency spectrum of Timoshenko beams", *J. Sound Vib.* **51** (1977), 123–137.

[Anderson 1953] R. A. Anderson, "Flexural vibration of uniform beams according to the Timoshenko theory", *J. Appl. Mech.* (*ASME*) **75** (1953), 504–510.

[Cooper 1966] G. R. Cooper, "The shear coefficient in Timoshenko's beam theory", *J. Appl. Mech.* (*ASME*) **33** (1966), 335–340.

[Demarest 1971] H. H. Demarest, Jr., "Cube resonance method to determine the elastic constants of solids", *J. Acoust. Soc. Am.* **49** (1971), 768–775.

[Dolph 1954] C. L. Dolph, "On the Timoshenko theory of transverse beam vibrations", *Quart. Appl. Math.* **12** (1954), 175–187.

[Gruttmann and Wagner 2001] F. Gruttmann and W. Wagner, "Shear correction factors in Timoshenko's beam theory for arbitrary shaped cross-sections", *Comput. Mech.* **27** (2001), 199–207.

[Han et al. 1999] S. M. Han, H. Benaroya, and T. Wei, "Dynamics of transversely vibrating beams using four engineering beam theories", *J. Sound Vib.* **225** (1999), 935–988.

[Herrmann 1955] G. Herrmann, "Forced motions of Timoshenko beam theory", *J. Appl. Mech.* (*ASME*) **77** (1955), 53–56.

[Hodges 2006] D. H. Hodges, *Nonlinear composite beam theory for engineers*, American Institute of Aeronautics and Astronautics, Reston, VA, 2006.

[Huang 1961] T. C. Huang, "The effect of rotatory inertia and of shear deformation on the frequency and normal mode equations of uniform beams with simple end conditions", *J. Appl. Mech.* (*ASME*) **28** (1961), 579–584.

[Hutchinson 2001] J. R. Hutchinson, "Shear coefficients for Timoshenko beam theory", *J. Appl. Mech.* (*ASME*) **68** (2001), 87–92.

[Hyer 1998] M. W. Hyer, *Stress analysis of fiber-reinforced composite materials*, McGraw-Hill, Boston, 1998.

[King 1985] J. L. King, "The free transverse vibrations of anisotropic beams", *J. Sound Vib.* **98** (1985), 575–585.

[Ledbetter et al. 1989] H. M. Ledbetter, S. K. Datta, and T. Kyono, "Elastic constants of a graphite-magnesium composite", *J. Appl. Phys.* **65** (1989), 3411–3416.

[Levinson 1981] M. Levinson, "A new rectangular beam theory", *J. Sound Vib.* **74** (1981), 81–87.

[Love 1927] A. E. H. Love, *A treatise on the mathematical theory of elasticity*, 4th ed., Dover, New York, 1927.

[Marigo and Meunier 2006] J.-J. Marigo and N. Meunier, "Hierarchy of one-dimensional models in nonlinear elasticity", *J. Elasticity* **83**:1 (2006), 1–28.

[Migliori and Sarrao 1997] A. Migliori and J. L. Sarrao, *Resonant ultrasound spectroscopy: applications to physics, materials measurements and non-destructive evaluation*, Wiley, New York, 1997.

[Ohno 1976] I. Ohno, "Free vibration of a rectangular parallelepiped crystal and its application to determination of elastic constants of orthorhombic crystals", *J. Phys. Earth* **24** (1976), 355–379.

[Pagano 1969] N. Pagano, "Exact solutions for composite laminates in cylindrical bending", *J. Compos. Mater.* **3** (1969), 398–411.

[Puchegger et al. 2003] S. Puchegger, D. Loidl, K. Kromp, and H. Peterlik, "Hutchinson's shear coefficient for anisotropic beams", *J. Sound Vib.* **266** (2003), 207–216.

[Puchegger et al. 2005] S. Puchegger, D. Loidl, K. Kromp, H. Peterlik, and R. Weiss, "Extension of the resonant beam technique to highly anisotropic materials", *J. Sound Vib.* **279** (2005), 1121–1129.

[Schramm et al. 1994] U. Schramm, L. Kitis, W. Kang, and W. D. Pilkey, "On the shear deformation coefficient in beam theory", *Finite Elem. Anal. Des.* **16** (1994), 141–162.

[Stephen 1978] N. G. Stephen, "On the variation of Timoshenko's shear coefficient with frequency", *J. Appl. Mech.* (*ASME*) **45** (1978), 695–697.

[Stephen 2001] N. G. Stephen, "Discussion of Hutchinson's paper shear coefficients for Timoshenko beam theory", *J. Appl. Mech.* (*ASME*) **68** (2001), 959–960.

[Thomas and Abbas 1975] J. Thomas and B. A. H. Abbas, "Finite element model for dynamic analysis of Timoshenko beam", *J. Sound Vib.* **41** (1975), 291–299.

[Timoshenko 1921] S. P. Timoshenko, "On the correction for shear of the differential equation for transverse vibrations of bars of uniform cross-section", *Philos. Mag.* **41** (1921), 744–746.

[Timoshenko 1922] S. P. Timoshenko, "On the transverse vibrations of bars of uniform cross-section", *Philos. Mag.* **43** (1922), 125–131.

[Timoshenko 1953] S. P. Timoshenko, *History of strength of materials*, Dover, New York, 1953.

[Traill-Nash and Collar 1953] R. W. Traill-Nash and A. R. Collar, "The effects of shear flexibility and rotatory inertia on the bending vibrations of beams", *Quart. J. Mech. Appl. Math.* **6** (1953), 186–222.

[Visscher et al. 1991] W. M. Visscher, A. Migliori, T. M. Bell, and R. A. Reinert, "On the normal modes of free vibration of inhomogeneous and anisotropic elastic objects", *J. Acoust. Soc. Am.* **90** (1991), 2154–2162.

Received 2 Jul 2012. Revised 15 Nov 2012. Accepted 13 Jan 2013.

PAUL R. HEYLIGER: prh@engr.colostate.edu
Department of Civil and Environmental Engineering, Colorado State University, Fort Collins, CO 80523-1372, United States

JOURNAL OF MECHANICS OF MATERIALS AND STRUCTURES

msp.org/jomms

Founded by Charles R. Steele and Marie-Louise Steele

Cover photo: Ev Shafrir

See msp.org/jomms for submission guidelines.

JoMMS (ISSN 1559-3959) at Mathematical Sciences Publishers, 798 Evans Hall #6840, c/o University of California, Berkeley, CA 94720-3840, is published in 10 issues a year. The subscription price for 2013 is US $555/year for the electronic version, and $705/year (+$60, if shipping outside the US) for print and electronic. Subscriptions, requests for back issues, and changes of address should be sent to MSP.

JoMMS peer-review and production is managed by EditFLOW® from Mathematical Sciences Publishers.

PUBLISHED BY

mathematical sciences publishers

nonprofit scientific publishing

http://msp.org/

Journal of Mechanics of Materials and Structures

Volume 8, No. 1 January 2013

Numerical and experimental investigation of the dynamic characteristics of cable-supported barrel vault structures SUN GUO-JUN, CHEN ZHI-HUA and RICHARD W. LONGMAN 1

When beam theories fail PAUL R. HEYLIGER 15

Transient 3D singular solutions for use in problems of prestressed highly elastic solids LOUIS MILTON BROCK 37

Wave velocity formulas to evaluate elastic constants of soft biological tissues PHAM CHI VINH and JOSE MERODIO 51

Tubular aluminum cellular structures: fabrication and mechanical response RYAN L. HOLLOMAN, VIKRAM DESHPANDE, ARVE G. HANSSEN, KATHERINE M. FLEMING, JOHN R. SCULLY and HAYDN N. G. WADLEY 65

Reflection of plane longitudinal waves from the stress-free boundary of a nonlocal, micropolar solid half-space AARTI KHURANA and SUSHIL K. TOMAR 95

1559-3959(2013)8:1;1-B